

# **Instability of Ultra-Thin Water Films and the Mechanism of Droplet Formation on Hydrophilic Surfaces**

A. Majumdar

Department of Mechanical Engineering  
University of California, Berkeley, CA 94720

I. Mezic

Department of Mechanical Engineering  
University of California, Santa Barbara, CA 93106

## **Abstract**

This paper presents a new theory of droplet formation during condensation of water on a hydrophilic surface. The theory uses hydration, electrostatic, van der Waals, and elastic strain interactions between a hydrophilic solid surface and a water film, and shows that contributions to the disjoining pressure are dominated by hydration forces for films thinner than 3 nm. The equilibrium film thickness is found to remain almost constant at about 0.5 nm for a wide range of relative humidity, although it increases sharply as the relative humidity approaches unity. The competition between strain energy on one hand, and hydration, van der Waals, and liquid-vapor surface tension on the other, induces instability for films thicker than a critical value. The critical wavelength of instability,  $L_{cr}$ , is also predicted as a function of film thickness. The theory proposes that as the relative humidity increases, nucleation initially occurs in monolayer fashion due to strong hydration forces. Using nucleation thermodynamics it predicts a critical nucleus size,  $d^*$ , and internuclei spacing,  $\ell$ , as a function of subcooling,  $DT$ , of the solid surface and shows that both length scales decrease with increasing subcooling. Since these monolayer nuclei are formed on the adsorbed water film, it is shown that when the internuclei spacing is larger than the critical wavelength,  $\ell > L_{cr}$ , instability occurs in the film resulting in droplet formation. The theory predicts that beyond a certain value of subcooling, the interdroplet spacing is “choked” and cannot decrease further.

## Nomenclature

$a$	elastic strain at liquid-solid interface
$A$	Hamaker constant [J]
$b$	thickness of a water monolayer [m]
$B$	height perturbation in liquid film [m]
$d$	radius of a critical water nucleus [m]
$e$	charge of an electron, $1.6 \times 10^{-19}$ [C]
$E$	elastic modulus [ $\text{N/m}^2$ ]
$g_v$	volumetric Gibb's free energy [ $\text{J/m}^3$ ]
$G$	Gibb's free energy [J]
$h$	film thickness [m]
$h_{fg}$	enthalpy of vaporization of water [J/kg]
$k_B$	Boltzmann constant, $1.38 \times 10^{-23}$ [J/K]
$\ell$	internuclei spacing [m]
$L$	length [m]
$P$	disjoining pressure [ $\text{N/m}^2$ ]
$P_v$	vapor pressure [ $\text{N/m}^2$ ]
$R$	gas constant for water vapor [J/kg-K]
$S$	supersaturation
$T$	temperature [K]
$U$	free energy parameter in hydration energy [ $\text{J/m}^2$ ]
$v$	valence
$w$	free energy per unit area [ $\text{J/m}^2$ ]
$W$	free energy [J]
$\epsilon$	dielectric constant
$\epsilon_0$	permittivity of vacuum, $8.85 \times 10^{-12}$ [ $\text{C}^2/\text{N}\cdot\text{m}^2$ ]
$h$	nucleation density [ $\text{m}^{-2}$ ]
$k$	reciprocal of Debye length [ $\text{m}^{-1}$ ]
$l$	length scale parameter in hydration energy [m]
$y$	relative humidity
$r$	ion concentration [ $\text{m}^{-3}$ ]
$f_0$	surface potential [V]
$c$	surface charge density [ $\text{C/m}^2$ ]
$s$	surface tension [ $\text{J/m}^2$ ]
$u$	volume of a water molecule [ $\text{m}^3$ ]

### Subscripts

$cr$	critical
$el$	electrostatic
$eq$	equilibrium
$hyd$	hydration
$lv$	liquid-vapor
$s$	surface
$sat$	saturation
$sr$	strain
$v$	volume
$vdW$	van der Waal

## 1. Introduction

Formation of droplets during condensation is a well-known phenomenon. Dropwise condensation provides some of the highest known heat transfer coefficients ( $\approx 10^4 - 10^5 \text{ W/m}^2 - \text{K}$ ) and is critical for many applications of technological importance such as heat exchangers. The normal procedure to promote dropwise condensation is to coat the surface with a hydrophobic or non-wetting material. However, dropwise condensation is not limited to non-wetting surfaces and has often been observed on hydrophilic or wetting surfaces. A common example is the fogging of glasses when one enters a warm room from a cooler exterior or when one breathes on a cold glass surface. Despite the wide use and observations of dropwise condensation, the underlying physics of droplet formation at the molecular scales is not well understood. A deeper understanding could of the mechanism of droplet formation could lead to surfaces whose chemistry is tailored for controlled dropwise condensation.

Several theories have been proposed which can be grouped in two categories. Jakob (1936) first proposed that condensation initially occurs in a film-wise manner. On reaching a critical thickness, the film ruptures and the liquid is drawn into droplets by surface tension. The experimental observations of Baer and McKelvey (1958), Welch and Westwater (1961), and Sugawara and Katsuta (1966) seem to confirm this school of thought. A different theory was proposed by Eucken (1937) who suggested that droplet formation is fundamentally a heterogeneous nucleation process of a liquid on a bare solid surface. When vapor molecules adsorb on a solid surface, they diffuse and form a critical nucleus that grows in time due to further condensation. The size of the critical nucleus depends on the liquid surface tension, the contact angle between the solid and the liquid droplet as well as the Gibbs free energy change during condensation. Experiments by Umur and Griffith (1965) and Erb and Thelen (1965) tend to support this theory. Although droplet formation has been a topic of study for over six decades, its origin has remained a topic of debate. Recent experiments on the nature of liquids in contact with solid surfaces have led to several key insights about the underlying intermolecular forces. These insights were not available when the first theories of dropwise condensation were proposed and have not yet been used to understand or explain the phenomenon. The purpose of this paper is to use this new knowledge of intermolecular forces and develop a new theory of droplet formation.

Insight about droplet formation can be obtained from studying the growth of solid films deposited on a solid surface. Three types of growth have been observed (Vook, 1982; Ohring, 1992). First is *island formation* due to heterogeneous nucleation of droplets. This occurs when the attractive forces between the adsorbed atoms and the substrate is less than that between two adsorbed atoms, and when the adsorbed atoms are sufficiently mobile to form nuclei. This is analogous to the Euken theory of water droplet formation. Second is *epitaxial* growth of solid films which happens when the adsorbed atoms are highly mobile and when the attractive forces between adsorbed atoms and the substrate are very strong. Third is *Stranski-Krastanov* growth in which the film initially grows epitaxially, but on reaching a critical thickness buckles into islands through instability in the film. The instability is induced by competition between elastic strain energy in the film caused by a mismatch in lattice constants, and the surface energy of the film surface which tries to reduce the film surface area (Srolovitz, 1989; Spencer et al., 1991). Beyond a critical thickness, elastic strain overwhelms surface tension resulting in film instability. Since strain energy depends on the film volume and surface energy depends on the surface area, their ratio produces a length scale, which is the critical thickness of the film. It will be shown here that droplet formation in water films on a hydrophilic solid surface is similar to Stranski-Krastanov growth of solid films. However, since the behavior of liquids is quite different from that of solids, there are several new aspects that will be presented here.

The paper will rely only on thermodynamic arguments leaving kinetics to a later study. The discussion will concentrate on condensation of water on a hydrophilic surface such as glass, although it can be extended to other types of surfaces as well, including hydrophobic ones. To simplify matters and to concentrate on the effect surface chemistry, it is assumed that the surface is atomically flat such that surface roughness effects can be neglected. Such a situation can be experimentally obtained on a mica surface.

## **2. Intermolecular Forces at Liquid-Solid Interfaces**

There are four types of intermolecular forces that exist between a solid hydrophilic surface and an adsorbed water film - hydration, electrostatic, van der Waals forces, and elastic strain. They operate at different length scales. To appreciate the role of all the forces, one must understand their nature in order to develop a model of water condensation from the molecular level.

2.1 Hydration Forces Solid surfaces such as silica, mica or any other oxides or hydrocarbons that contain a polar group, are hydrophilic and form hydrogen bonds with water. The H-bond strength between water molecules and the surface can be so strong that the first few layers of water completely wet the surface and are often highly structured. This is described qualitatively in Fig. 1, which shows the oscillating density profile near a rigid surface. Such density profiles have been theoretically predicted or obtained by computer simulations (Marcelja et al., 1976; Marcelja and Radic, 1976; Abraham, 1978; Snook and van Megen, 1979; Jonsson, 1981; Xia and Berkowitz, 1995). The H-bonding network is quite extensive in range and the interfacial force between the hydrophilic surface and the water layer can be long range (Stanley and Teixeira, 1980).

Experimental evidence of such highly ordered 2-dimensional phase of water has been obtained by several investigators. Israelachvili and Pashley (1983) used the surface force apparatus (SFA) to bring into contact two cylindrical pieces of mica with the cylinder axes perpendicular to each other. The force between the two cylinders was measured as a function of the distance between them. Figure 2a shows a plot of the force-distance diagram that clearly exhibits the oscillating hydration forces. The period of oscillation is about 0.25 nm which is roughly equal to the diameter of a water molecule. There is also an exponential decay of the force envelope with a characteristic length,  $l$ , of about 1-2 nm. Therefore, the 2-dimensional phase of water near a mica surface can extend 3-10 monolayers.

The oscillatory behavior of the hydration forces is primarily caused due to the crystalline nature of the contacting surfaces. If the surfaces are non-crystalline, such as in glass or fused silica, or if the surfaces are slightly rough, then the oscillatory forces are not observed (Horn et al, 1989) but the strong repulsion between the surfaces and the exponential decay of hydration forces

are still detected, as evident in Fig. 2b. For a film thickness,  $h$ , Israelachvili (1992) proposed that the hydration energy can be written as

$$w_{hyd}(h) = U \exp\left(-\frac{h}{I}\right) \quad (1)$$

Typically,  $I$  is on the order of 1 nm and  $U$  ranges from 3-30 mJ/m<sup>2</sup>. Such a relation cannot be derived from first principles but is a close fit to experimental observations. It does not account for the oscillatory nature observed in Fig. 2a but provides the average energy characteristic of that observed in Fig. 2b. However, it should be noted although equation (1) suggests that hydration energy asymptotes to a finite value as  $h \rightarrow 0$ , experimental data show that the hydration energy keeps increasing as the film thickness decreases. In view of this fact, it is proposed here that the hydration energy is

$$w_{hyd}(h) = U \left(1 + \frac{I}{h}\right) \exp\left(-\frac{h}{I}\right) \quad (2)$$

This retains the exponential behavior for film thickness on the order of  $I$  but introduces a  $1/h$  behavior for thinner films. Note that a generic polynomial,  $h^{-n}; n > 1$ , can be chosen but the results of the stability analysis obtained later will not significantly change. Hence, the  $h^{-1}$  behavior is chosen for simplicity.

**2.2 Electrostatic Forces** Electrostatic forces play a strong role in long-range interactions between water films and a solid surface. A solid surface can be charged in two ways: (i) by ionization or dissociation of a surface group - for example, removal of K<sup>+</sup> ions from a mica surface; (ii) adsorption of ions from solution to a previously uncharged surface - for example adsorption of Ca<sup>2+</sup> ions from solution to replace the K<sup>+</sup> ions in mica. Note that even pure water dissociates into an ionic solution of H<sub>3</sub>O<sup>+</sup> and OH<sup>-</sup>. When a surface is charged, a region of oppositely charged counterions in solution are attracted to the surface. The charge density of counterions decreases with distance from the surface and approaches the bulk value far away. The combination of surface charge and counterions in solution forms a region near the surface called the *electric double layer*. The only reason the ions in the solution do not collapse onto the charged surface is due to rapid thermal motion, which creates a repulsive pressure.

There has been extensive research on quantifying the potential energy of a water film that is electrostatically bound to a solid surface. An excellent description can be found in Israelachvili (1992). The relation between surface charge density,  $\mathbf{c}$ , and surface potential,  $\mathbf{f}_o$ , can be found from the Grahame equation

$$\mathbf{c} = \sqrt{2\mathbf{e}\mathbf{e}_o k_B T \left( \sum_i \mathbf{r}_{oi} - \sum_i \mathbf{r}_{\infty i} \right)} \quad (3)$$

where  $\mathbf{e}$  is the dielectric constant of the medium which in our case is water,  $\mathbf{e}_o$  is the permittivity of vacuum,  $k_B$  is the Boltzmann constant,  $T$  is the temperature, and  $\mathbf{r}_{oi}$  and  $\mathbf{r}_{\infty i}$  are the ion concentrations at the surface and far away in solution, respectively, for the  $i$ th type of ions. These concentrations are related as

$$\mathbf{r}_{oi} = \mathbf{r}_{\infty i} \exp\left(-\frac{v_i e \mathbf{f}_o}{k_B T}\right) \quad (4)$$

where  $v_i$  is the valence of the ions. Therefore, knowledge of all the bulk ion concentrations in solution,  $\mathbf{r}_{\infty i}$ , and the surface charge density,  $\mathbf{c}$ , can be used to determine the surface potential,  $\mathbf{f}_o$ . For sufficiently small values of  $\mathbf{f}_o$ , i.e.  $\mathbf{f}_o < 25$  mV, the Grahame equation reduces to

$$\mathbf{c} = \mathbf{e}\mathbf{e}_o \mathbf{k} \mathbf{f}_o \quad (5)$$

where  $1/\mathbf{k}$  is called the Debye length or characteristic thickness of the electric double layer and  $\mathbf{k}$  is given as

$$\mathbf{k} = \sqrt{\sum_i \frac{\mathbf{r}_{\infty i} e^2 v_i^2}{\mathbf{e}\mathbf{e}_o k_B T}} \quad (6)$$

The potential energy of the system (water film and solid surface) can be derived from these results. Consider a single specie of ions present in the water film. For a film of thickness  $h$ , the potential energy density of the system is (Israelachvili, 1992)

$$w_{el}(h) = \frac{64k_B T \mathbf{r}_{\infty} \mathbf{g}^2}{\mathbf{k}} \exp(-\mathbf{k}h) \quad (7)$$

where  $\mathbf{r}_{\infty}$  is the concentration of the solution far away from the surface and  $\mathbf{g}$  is given by

$$\mathbf{g} = \tanh\left(\frac{e \mathbf{f}_o}{4k_B T}\right) \quad (8)$$

Note that the influence of the electrostatic forces depends on the Debye length,  $1/k$ . For a NaCl solution, this 30.4 nm at  $10^{-4}$  M concentration, 9.6 nm at 1 mM and 0.3 nm at 1 M. For pure water at pH 7, the Debye length is 960 nm or about 1  $\mu\text{m}$ . Therefore, the electrostatic forces can be much longer range than the hydration forces.

2.3 van der Waals Forces Although not as strong as hydration or electrostatic forces, van der Waals forces are always present whenever a liquid is adsorbed onto a surface. They arise from interactions of induced dipoles between two or more atoms and are typically effective below 10-50 nm. There is extensive literature on van der Waals forces between an adsorbed water film and a surface in the presence of vapor. The interaction energy density is written as

$$w_{vdW}(h) = -\frac{A}{12ph^2} \quad (9)$$

where  $A$  is the Hamaker constant which depends on the optical properties of the three media - solid surface, water film and the vapor. Values of the Hamaker constants for several combinations have been calculated and listed in Israelachvili (1992). For example, for a system of water adsorbed on fused quartz in the presence of air,  $A = -0.87 \times 10^{-20}$  J. A negative value of  $A$  suggests that the energy of the system will reduce if the film grows thicker.

2.4 Elastic Strain The fact that water molecules are highly ordered in a two-dimensional ice-like structure close to a hydrophilic surface has been established through experiments and molecular dynamic simulations. Therefore, if the lattice constant of the substrate is not exactly equal to that of ice, the bonds between the water molecules will be strained. The fact that strain influences phenomena at the solid-liquid interface has been known for a while. For example, silver iodide (AgI) has been used to nucleate ice and it is commonly believed that it is the lattice match of the crystal structure of AgI and ice that promotes ice nucleation (Hobbs, 1974). Recent experiments have also shown that strain energy can play a significant role in nucleation processes, in particular for heterogeneous nucleation of ice from water on a solid surface (Gavish et al., 1990; Majewski et al., 1993; Popovitz-Biro et al., 1994). In addition, a recent experiment showed that the first few layers of liquid mercury in contact with a diamond surface form layered structure with the orientation of solid-Hg crystal (Huisman et al., 1997). Hence, if the first few layers are solid-like,



there should be some strain due to mismatch in the lattice constants of the solid-like liquid film in contact with the solid substrate. Note, however, that in bulk liquid water, there is no strain between the water molecules. Since the origin of the layered structure lies in hydration forces which decay exponentially, it is proposed here that the strain energy density (per unit volume) at any point in the film is equal to  $Ea^2e^{-h/l}/2$  where  $E$  is the elastic modulus of ice which is 17 GN/m<sup>2</sup> (Turnbull and Vonnegut, 1952) and  $a$  is the strain of the first monolayer. Values of  $a$  typically range between 0 and 5 percent. Hence, total elastic strain energy surface density (per unit film area) of a film of thickness,  $h$ , varies as

$$w_{sr} = \frac{EIa^2}{2} \left[ 1 - \exp\left(-\frac{h}{l}\right) \right] \quad (10)$$

where  $E$  is the elastic modulus of ice which is 17 GN/m<sup>2</sup> (Turnbull and Vonnegut, 1952).

### 3. Equilibrium Thickness of Water Films

The total energy density of the system is obtained by adding up the interaction energies as follows

$$w = w_{hyd} + w_{el} + w_{vdW} + w_{sr} \quad (11)$$

It should be noted that when only electrostatic and van der Waals forces are considered, the celebrated DLVO theory results, after Derjaguin and Landau (1941) and Verwey and Overbeek (1948). However, the experiments in Fig. 2 clearly show that hydration must be taken into account for films thinner than a 2-3 nm. In previous studies of liquid films undergoing evaporation or condensation or under equilibrium, only the van der Waals interactions were included whereas electrostatic and hydration energies were neglected (Bankoff, 1990; Burelbach et al., 1988; Wayner et al., 1976; Dasgupta et al., 1994). Although these studies concentrated on thicker films for which this may be acceptable, it is not realistic to do so for films in the range of 0-10 nm. This will be demonstrated now.

The disjoining pressure for the water film can be calculated as

$$P(h) = -\frac{dw}{dh} = \frac{Ue^{-h/l}}{l} \left( 1 + \frac{h}{l} + \frac{l^2}{h^2} \right) + 64k_B T r_\infty g^2 e^{-kh} - \frac{A}{6ph^3} - \frac{Ee_o^2}{2} e^{-h/l} \quad (12)$$

where the four terms on the right side represent the contributions from hydration, electrostatic, van der Waals, and strain interactions. It is important to compare the contribution of the three interactions to the disjoining pressure. This is depicted in Fig. 3 where calculations are presented for  $T = 300$  K and some typical parameters are assumed -  $l = 1$  nm and  $U = 10$  mJ/m<sup>2</sup> for hydration;  $A = -10^{-20}$  J for van der Waals interaction; and for electrostatic interactions four NaCl electrolyte concentrations,  $10^{-7}$  M (pure water),  $10^{-4}$  M,  $10^{-2}$  M and 1 M, are assumed. In addition, it is assumed that the surface potential is  $\phi_0 = 100$  mV for a electrolyte solution of NaCl. The Debye length varies as  $1/k = 0.304/\sqrt{[NaCl]}$  nm where  $[NaCl]$  is the molar concentration.

It is clear from Fig. 3 that for pure water ( $10^{-7}$  M), hydration interactions dominate for  $h < 10$  nm and van der Waals dominate in the range  $h > 10$  nm. For  $10^{-4}$  M concentration of NaCl, hydration force is the largest for  $h < 7$  nm whereas for thicker films, electrostatic forces dominate. van der Waals forces are insignificant for such a condition. For  $10^{-2}$  M, hydration dominates for  $h < 3$  nm whereas electrostatic forces dominate for thicker films. For 1 M, though, electrostatic forces decay very quickly and become insignificant making this case similar to that of  $10^{-7}$  M where only hydration and van der Waals forces are important.

The disjoining pressure can also be related to the relative humidity,  $\mathbf{y}$ , as follows (Israelachvili, 1992)

$$P(h) = -\frac{dw}{dh} = \frac{k_B T}{\mathbf{u}} \ln\left(\frac{1}{\mathbf{y}}\right) \quad (13)$$

Here  $\mathbf{u}$  is the volume of a water molecule ( $\approx 3 \times 10^{-29}$  m<sup>3</sup>). The disjoining pressure from equation (12) can be used in equation (13) to establish a relation between the equilibrium film thickness,  $h_{eq}$ , and the relative humidity,  $\mathbf{y}$ . Figure 4 shows such a plot. For humidity below 90 percent,  $h_{eq}$  is less than 1 nm. In this regime, hydration forces are dominant. This is also clear from Fig. 4, which shows that electrolyte concentrations have negligible effect on  $h_{eq}$ . This further emphasizes the point that hydration forces must be included in the analysis of evaporation and condensation of the water film. It is interesting to note that the equilibrium film thickness does not change appreciably over a wide range of relative humidity. The inset in Fig. 4 shows,

however, that when the humidity reaches close to 100 percent, the equilibrium film thickness increases sharply. It will be established in section 4 that during this increase in film thickness, the film becomes unstable and undergoes a transition to droplet formation.

To qualitatively demonstrate the existence of the water film, Fig. 5 presents some results of an experiment performed using an atomic force microscope (AFM). A sharp tip made of silicon nitride was brought in contact with a freshly-cleaved mica surface and the cantilever deflection was measured with a laser. Figure 5a plots the cantilever deflection as a function of sample position, indicating in the inset the jump-to-contact phenomenon when the tip is within a few nanometers from the surface. This occurs when the attractive force between the two liquid films on the tip and the mica surface exceeds the spring force of the AFM cantilever. When the sample is retracted, notice that the tip sticks to the surface (6-7-8) until the spring force exceeds the force between the water films. Figure 5b plots jump-to-contact distance as a function of relative humidity. The fact that this increases with humidity suggests that the water film increases in thickness with humidity. It is difficult to determine the exact film thickness from this experiment, but the data qualitatively demonstrates the presence of the water film and its growth with increasing relative humidity.

#### 4. Onset of Liquid Film Instability

Consider a thin liquid film of thickness,  $h_o$ , on a flat surface. A one-dimensional disturbance to film changes the shape to  $h(x) = h_o + B \cos(\pi x/L)$  where  $B$  is a small perturbation and  $2L$  is the wavelength, as shown in Fig. 6. Such a profile conserves mass since

$$\int_0^L h(x) dx = h_o L \quad (14)$$

The total change in the film free energy can be written as

$$DW = DW_v + DW_s \quad (15)$$

where  $DW_v$  is the volumetric component and  $DW_s$  is the surface component. The change in volumetric free energy per unit length can be found as

$$DW_v = \int_0^L \frac{dw_v}{dh} \Big|_{h_o} (h - h_o) dx + \int_0^L \frac{d^2 w_v}{dh^2} \Big|_{h_o} \frac{(h - h_o)^2}{2} dx + \dots \quad (16)$$

Due to mass conservation, the first term on the right side is zero. Using the cosine profile of the film thickness and neglecting terms higher than the second order term, equation (16) becomes

$$DW_v = \frac{d^2 w_v}{dh^2} \Big|_{h_o} \frac{B^2 L}{4} \quad (17)$$

It will be assumed here that electrostatic forces are negligible. As Fig. 3 indicates, for film thicknesses less than 3 nm, electrostatic forces are not dominant even for surface potential of 100 mV. For lower surface potential, electrostatic forces will be even less. Hence, the volumetric energy density consists of van der Waals, hydration, and strain energy in the liquid film and can be written as

$$w_v = -\frac{A}{12ph^2} + U \left( 1 + \frac{I}{h} \right) \exp\left(-\frac{h}{I}\right) + \frac{E I e_o^2}{2} \left[ 1 - \exp\left(-\frac{h}{I}\right) \right] \quad (18)$$

Thus, the total change in volumetric free energy per unit length of the film can be derived to be

$$DW_v = \frac{B^2 L}{4} \left[ -\frac{A}{2ph^4} + \frac{U}{I^2} \left( 1 + \frac{I}{h} + \frac{2I^2}{h^2} + \frac{2I^3}{h^3} \right) \exp\left(-\frac{h}{I}\right) - \frac{E e_o^2}{2I} \exp\left(-\frac{h}{I}\right) \right] \quad (19)$$

Here, the subscript  $o$  has been dropped from the film thickness. To calculate the change in surface energy, it is necessary to calculate the change in surface area. Using the cosine profile, the change  $DL$  in the surface area is given as

$$DL = \int_0^L \sqrt{1 + \left( \frac{Bp}{L} \right)^2 \sin^2\left(\frac{px}{L}\right)} dx - L \quad (20)$$

Assuming that  $B \ll L$  (small perturbation), equation (20) can be simplified to

$$DL = 2 \left( \frac{Bp}{L} \right)^2 \int_0^L \sin^2\left(\frac{px}{L}\right) dx = \frac{(Bp)^2}{L} \quad (21)$$

Hence, the change in total surface energy due to the perturbation is

$$DW_s = \frac{s_{lv} (Bp)^2}{L} \quad (22)$$

where  $\mathbf{s}_{lv}$  is the surface tension for the liquid-vapor interface. Thus the total change in film free energy can be written as

$$DW = \frac{B^2 L}{4} \left[ -\frac{A}{2\mathbf{p}h^4} + \left\{ \frac{U}{I^2} \left( 1 + \frac{I}{h} + \frac{2I^2}{h^2} + \frac{2I^3}{h^3} \right) - \frac{E\mathbf{e}_o^2}{2I} \right\} \exp\left(-\frac{h}{I}\right) \right] + \frac{\mathbf{s}_{lv} B^2 \mathbf{p}^2}{L} \quad (23)$$

For the film to be stable, the total change in free energy must be greater than zero, i.e.  $DW > 0$ . It is clear that if only van der Waals and surface tension forces are considered, as has been done for most previous studies that considered thicker films (Bankoff, 1990; Burelbach et al., 1988; Wayner et al., 1976; Dasgupta et al., 1994), film instability will set in for wavelengths larger than the critical length,  $L_{cr}$ , given as

$$L > L_{cr}; \quad L_{cr} = h^2 \sqrt{\frac{8\mathbf{p}^3 \mathbf{s}_{lv}}{A}} \quad (24)$$

Short wavelength instabilities are not permitted due to surface tension forces. It is assumed here that the Hamaker constant,  $A$ , is positive. This is true in many cases (Israelachvili, 1992), including water on hydrophobic surfaces. In the case of negative Hamaker constant, such as for glass-water-air combination, the film is always stable as suggested by equation (23). Hence, for any film-droplet transition for water on glass, other forces must play a role. As observed in equation (23), hydration forces alone cannot be responsible since it has a positive coefficient. This suggests that strain energy must play an important role. After considering all the forces, the critical wavelength can be written as

$$L_{cr} = \sqrt{\frac{4\mathbf{s}_{lv}\mathbf{p}^2}{\frac{A}{2\mathbf{p}h^4} + \left[ \frac{E\mathbf{e}_o^2}{2I} - \frac{U}{I^2} \left( 1 + \frac{I}{h} + \frac{2I^2}{h^2} + \frac{2I^3}{h^3} \right) \right] \exp\left(-\frac{h}{I}\right)}} \quad (25)$$

It should be noted that so far there has been no assumption made whether the surface is hydrophobic or hydrophilic. This depends on the constants  $A$  and  $U$ . However, the theory developed till now can be used for both cases. As a case study, consider water on a hydrophilic surface such as glass in the presence of water vapor. As previous studies have indicated,  $U$  lies between 3-30 mJ/m<sup>2</sup> and  $I$  is about 1 nm. Hence, the parameters chose for this case study are:  $A$

$= -10^{-20}$  J (Israelachvili, 1992);  $U = 10$  mJ/m<sup>2</sup>;  $I = 1$  nm;  $E = 1.7 \times 10^{10}$  J/m<sup>2</sup>;  $a = 0.04$  (typical strain for lattice mismatch); and  $s_{lv} = 72$  mJ/m<sup>2</sup> (surface energy of liquid-vapor interface for water). Figure 7 plots  $1/L_{cr}$  as a function of film thickness and shows the stability boundary. The thickness steps taken for the calculation and represented as filled circles are 0.28 nm which is the size of a water monolayer. It is clear from Fig. 7 that for thickness larger than 3 nm, the film can become unstable. When compared with the plot of film thickness versus humidity in Fig. 4, it becomes apparent that when the relative humidity approaches 100 percent resulting in condensation, the water film becomes unstable.

## 5. Nucleation Phenomena

The analysis described above shows the stability regimes of thin liquid films. However, it provides no indication as to how the instability occurs and the subsequent shape of the liquid film. The following analysis will provide this insight.

Figure 7 shows that for a film of critical thickness,  $h_{cr}$ , instability will occur if the wavelength of oscillation,  $L_{cr}$ , is extremely large, i.e.,  $1/L_{cr} \rightarrow 0$ . Therefore, for all practical purposes, the film is stable when  $h = h_{cr}$ . However, if a single monolayer is added to the film, the critical wavelength,  $L_{cr}(h_{cr} + b)$ , reduces to about 0.4  $\mu\text{m}$  (see Fig. 7). Here,  $b$  is the size of a single water monolayer which is about 2.8  $\text{\AA}$ . Addition of another monolayer further reduces the critical wavelength to 0.3  $\mu\text{m}$ . Certainly, these wavelengths are possible under most physical conditions.

In light of the experimental evidence that water films form two-dimensional layered structures on a hydrophilic surface due to hydration forces, it is proposed that instability of a water film occurs in the following way. As the relative humidity increases, the equilibrium water film increases in thickness as indicated in Fig. 4. The water film remains stable till the thickness reaches the critical thickness,  $h_{cr}$ . If more condensation occurs, it is proposed that the water molecules stick to the water film in a two-dimensional monolayer fashion, as illustrated in Fig. 8. This is based on the recent experimental observations of Hu et al. (1995) who used the atomic

force microscope to image condensed water films on a mica surface with nanometer-scale spatial resolution. They observed that water nuclei are formed in two-dimensional monolayer fashion. Thermodynamics requires the existence of a critical nucleus of size,  $d^*$ , as will be shown next. Besides this, another length scale is the mean separation between critical nuclei,  $\ell$ . If it so happens that either  $d^* > L_{cr}(h_{cr} + b)$  or  $\ell > L_{cr}(h_{cr} + b)$ , then the film will undergo an instability since either  $\ell$  or  $d^*$  will fall within the unstable region of the stability map of Fig. 7. Since the mean separation between nuclei,  $\ell$ , is larger than the nucleus size, the condition  $\ell > L_{cr}(h_{cr} + b)$  is sufficient for instability.

Consider a two-dimensional circular nucleus of radius,  $d$ , formed from a single monolayer of height,  $b$ , as shown in Fig. 8. The change in Gibbs free energy for the formation of this nucleus is

$$\Delta G = -\mathbf{p}d^2b \left( \Delta g_v - \frac{Ee^2(h_{cr} + b)}{2} \right) + 2\mathbf{p}db\mathbf{s}_{lv} \quad (26)$$

where  $\mathbf{D}g_v$  is the reduction in volumetric Gibbs energy during condensation. The second term in the parenthesis is the strain energy increase for a monolayer at a height,  $h_{cr} + b$ , above the solid surface. Using  $d(\Delta G)/d(d) = 0$ , the critical nucleus size can be found to be

$$d^* = \frac{\mathbf{s}_{lv}}{\Delta g_v - \frac{Ee^2(h_{cr} + b)}{2}} \quad (27)$$

Using this in equation (26), the energy barrier to forming a critical nucleus can be found to be

$$\mathbf{D}G^* = \frac{\mathbf{p}b\mathbf{s}_{lv}^2}{\mathbf{D}g_v - Ee^2/2} \quad (28)$$

If  $\mathbf{h}_o$  is the density of possible nucleation sites, the nucleation density,  $\mathbf{h}$ , can be expressed as

$$\mathbf{h} = \mathbf{h}_o \exp\left(-\frac{\mathbf{D}G^*}{k_B T}\right) = \mathbf{h}_o \exp\left[-\frac{\mathbf{p}b\mathbf{s}_{lv}^2}{(\mathbf{D}g_v - Ee^2/2)k_B T}\right] \quad (29)$$

Therefore, the mean separation between nuclei follows as

$$\ell = \frac{1}{\sqrt{\mathbf{h}}} = b \exp \left[ \frac{pb\mathbf{s}_{lv}^2}{(2\mathbf{D}g_v - E\mathbf{e}^2)k_B T} \right] \quad (30)$$

where it is assumed that  $b = 1/\sqrt{\mathbf{h}_o}$ , i.e., the density of possible nucleation sites on the liquid film corresponds to the intermolecular distance.

Consider subcooling of a surface by  $\mathbf{DT} = T_{sat}(P_v) - T$ , where  $T_{sat}(P_v)$  is the saturation temperature at vapor pressure,  $P_v$ , and  $T$  is the temperature of the surface on which condensation takes place. Using the Clausius-Clapeyron equation, it can be shown that

$$S = \frac{P_v(T) - P_{sat}(T)}{P_{sat}(T)} = \exp \left[ \frac{h_{fg}}{R} \left( \frac{1}{T} - \frac{1}{T_{sat}(P_v)} \right) \right] - 1 \quad (31)$$

where  $S$  is called the vapor supersaturation,  $h_{fg}$  is the enthalpy of vaporization, and  $R$  is the gas constant for water vapor. If the subcooling is small, then  $S$  can be expressed as

$$S = \frac{h_{fg}}{RT^2} \mathbf{DT} \quad (32)$$

Using  $R = 461.38$  J/kg-K and  $h_{fg} = 2437.6$  kJ/kg at  $T = 300$  K for water, one obtains  $S = 0.059\mathbf{DT}$ . The reduction in volumetric Gibbs free energy can be related to vapor supersaturation as (Ohring, 1992)

$$\Delta g_v = \frac{k_B T}{\mathbf{u}} \ln(1 + S) \quad (33)$$

where  $\mathbf{u}$  is the volume of a water molecule which can be estimated as  $b^3$  or  $2.2 \times 10^{-29}$  m<sup>3</sup>.

It is clear from the above analysis that when the subcooling increases, vapor supersaturation ( $S$ ) increases resulting in an increase in  $\mathbf{D}g_v$ . This decreases the size of the critical nucleus,  $d^*$ , as well as the internuclei spacing,  $\ell$ . This is quantitatively shown in Fig. 9 which plots both  $\ell$  and  $d^*$  for water at a saturation temperature of 300 K. The values of  $E$ ,  $a$ , and  $\mathbf{I}$  are the same as used before for Fig. 7. It is interesting to note that for subcooling higher than 1 K, the critical nucleus size does not change appreciably and falls in the range of 1-10 nm. On the other hand, the internuclei separation is a strong function of subcooling and can vary over an order of magnitude for a change in subcooling by 1 K. Two other length scales - size of water



molecule and the minimum critical wavelength,  $L_{cr,min}$  — are also shown in Fig. 9. The critical nucleus size approaches the water molecule size as subcooling is increased and is always less than  $L_{cr,min}$ . Hence, instability occurs through the condition  $\ell > L_{cr}$  and not through the condition  $d^* > L_{cr}$ . However, note that when the subcooling increases above 9 K, the internuclei separation falls below  $L_{cr,min}$ . Although this would suggest that instability will not occur, there will always be sub-harmonics of the internuclei separation, i.e.,  $n\ell, n > 1$ , which will satisfy the condition that  $n\ell > L_{cr}$ . This means that every nuclei will not produce droplets, but those that are separated by internuclei distance of  $L_{cr}$  will induce instability and form droplets. Therefore, below subcooling of 9 K, the interdroplet separation will be equal to the internuclei separation since every nuclei will produce a droplet. For subcooling higher than 9 K, the interdroplet separation is “choked” and will not further decrease below  $L_{cr,min}$ .

Equation (23) suggests that the total change in film free energy can be written as  $DW = \mathbf{x}(h)B^2$ . For an unstable film,  $\mathbf{x}(h) < 0$ . The fact that  $DW \propto B^2$  suggests that once the instability occurs, the maximum reduction in energy is achieved when the film nuclei grow. Mass conservation demands that this can only happen when the film becomes thinner in internuclei region. This process is essential in the formation of droplets. The shape of the droplet requires further research on the surface energies and the contact angle, which has been left for a later study. In addition, the time it takes for this instability to occur depends on the kinetics of the process that have not been included in this study and, again, has been left for a later study.

It should be noted that since the internuclei spacing is larger than 1  $\mu\text{m}$  for subcooling less than 8 K, it would be possible to observe these nuclei under an optical microscope. Hence, an experiment of condensation of water on mica under controlled humidity and temperature conditions is now being planned. Comparison of the measured average internuclei spacing as a function of subcooling with the theoretical predictions in Fig. 9 would verify the theoretical predictions of the instability and nucleation theories presented in this paper.

## 6. Conclusions

This paper presents a new theory for instability of ultrathin water films on a hydrophilic surface that leads to the formation of droplets during condensation. Previous studies on instability have concentrated only on thicker films and included van der Waals and surface tension forces for analysis. However, previous experimental and theoretical studies have shown that for films thinner than about 3 nm, hydration forces dominate. In addition, electrostatic forces within the double layer as well as elastic strain of the water film near the solid surface are also important. Using all the known intermolecular interactions, the paper calculates the equilibrium film thickness as a function relative humidity and shows that the thickness is about 0.5 nm (2 monolayer) for a wide range of humidity but grows very sharply as the humidity approaches 100 percent. Using purely thermodynamic arguments, the stability theory shows that there exists a critical film thickness on about 3 nm such that thicker films can undergo an instability arising from a competition between strain energy on one hand, and van der Waals, hydration, and surface tension on the other. Once the critical film thickness is reached, further condensation results in the formation of nuclei of a critical size in a monolayer fashion. Based on the thermodynamics of nucleation, the critical nucleus size and the internuclei spacing are predicted as a function of surface subcooling. When the internuclei spacing is larger than the critical wavelength, the resulting instability leads to growth of the critical nuclei to form droplets. The theory predicts that although the interdroplet spacing decreases with increasing subcooling, the spacing “chokes” beyond a certain subcooling value and remains constant. In summary, the paper proposes a new theory of droplet formation during condensation of water on a hydrophilic surface. The theory has elements of both previous theories which propose either film instability or heterogenous nucleation as the mechanism for droplet formation.

## **Acknowledgments**

We thank Steve Morris and Van Carey for their insightful comments, and K. Ogawa for performing the AFM experiments. AM would like to thank the NSF for the NYI award under which this study was conducted.

## References

- Abraham, F. F., 1978, "The interfacial density profile of a Lennard-Jones fluid in contact with a (100) Lennard-Jones wall and its relationship to idealized fluid-wall systems," *J. Chem. Phys.*, Vol. 68(8), pp. 3713-3716.
- Baer, E. and McKelvey, J. M., 1958, "Heat transfer in dropwise condensation," *Proc. of Symp. On Heat Transfer in Dropwise Condensation*, p. 24., U. of Delaware, Newark.
- Bankoff, S. G., 1990, "Dynamics and stability of thin heated liquid films," *ASME J. Heat Trans.*, Vol. 112, pp. 538-545.
- Burelbach, J. P., Bankoff, S. G., and Davis, S. H., 1988, "Nonlinear stability of evaporating/condensing liquid films," *Journal of Fluid Mechanics*, Vol. 195, pp. 463-494.
- Dasgupta, S., Kim, I. Y. and Wayner, P. C. Jr., 1994, "Use of Kelvin-Claapeyron equation to model an evaporating curved microfilm," *ASME J. Heat Transfer*, Vol. 116, pp. 1007-1015.
- Derjaguin, B. V. and Landau, L., 1941, *Acta Physicochim. URSS*, Vol. 14, pp. 633-662.
- Erb, R. A. and Thelen, E., 1965, "Dropwise condensation," 1<sup>st</sup> Int. Symp on Water Desalination, Washington DC. Also Erb, R. A., PhD Diss., Temple Univ. (1965).
- Eucken, A., 1937, *Naturwissenschaften*, Vol. 25, p. 209.
- Gavish, M., Popovitz-Biro, R., Lahav, M. and Leiserowitz, L., 1990, "Ice nucleation by alcohols arranged in monolayers at the surface of water drops," *Science*, Vol. 250, pp. 973-975.
- Hobbs, P. V., 1974, *Ice Physics*, Clarendon Press, Oxford.
- Horn, R. G., Smith, D. T., and Haller, W., 1989, "Surface forces and viscosity of water measured between silica sheets," *Chemical Physics Letters*, Vol. 162(4,5), pp. 404-408.
- Hu, J., Xiao, X. D., Ogletree, D. F. and Salmeron, M., 1995, "Imaging the condensation and evaporation of molecularly thin films of water with nanometer resolution," *Science*, Vol. 268, pp. 267-269.
- Huisman, W. J.; Peters, J. F.; Zwanenburg, M. J.; deVries, S. A.; Derry, T. E.; Abernathy, D., and vanderVeen, J. F., 1997, "Layering of a liquid metal in contact with a hard wall," *Nature*, Vol. 390(6658), pp. 379-381.
- Israelachvili, J. N., 1992, *Intermolecular and Surface Forces*, 2<sup>nd</sup> Ed., Academic Press, San Diego.

Israelachvili, J. N. and Pashley, R. M., 1983, "Molecular layering of water at surfaces and origin of repulsive hydration forces," *Nature*, Vol 306, pp. 249-250.

Jakob, M. 1936, *Mech. Engr.*, Vol. 58, pp. 729-

Jonsson, B., 1981, "Monte Carlo simulations of liquid water between two rigid walls," *Chem.Phys. Lett.*, Vol. 82(3), pp. 520-525.

Majewski, J., Popovitz-Biro, R., Kjaer, K., Als-Neilsen, J., Lahav, M. and Leiserowitz, L., 1994, "Toward a determination of the critical size of ice nuclei. A demonstration by grazing incidence X-ray diffraction of epitaxial growth of ice under the C<sub>31</sub>H<sub>63</sub>OH monolayer," *J. Phys. Chem.*, Vol. 98, pp. 4087-4093.

Marcelja, S. and Radic, N., 1976, "Repulsion of interfaces due to boundary water," *Chemical Physics Letters*, Vol. 42(1), pp. 129-130.

Marcelja, S., Mitchell, D. J., Ninham, B. W., and Sculley, M. J., 1976, "Role of solvent structure in solution theory," *J. Chem. Soc. Faraday Trans. 2*, Vol. 73, pp. 630-648.

Ohring, M., 1992, *The Materials Science of Thin Films*, Academic Press, San Diego.

Popovitz-Biro, P., Wang, J. L., Majewski, J., Shavit, E., Leiserowitz, L. and Lahav, L., 1994, "Induced freezing of supercooled water into ice by self-assembled crystalline monolayers of amphiphilic alcohols at the air-water interface," *J. Am. Chem. Soc.*, Vol. 116, pp. 1179-1191.

Snook, I and van Megen, W., 1979, "Structure of dense liquids at solid interfaces," *J. Chem. Phys.*, Vol. 70(6), pp. 3099-3105.

Spencer, B. J., Voorhees, P. W., and Davis, S. H., 1991, "Morphological instability in epitaxially strained dislocation-free solid films," *Physical Review Letters*, Vol. 67(26), pp. 3696-3699.

Srolovitz, D. J., 1989, "On the stability of surfaces of stressed solids," *Acta metall.*, Vol. 37(2), pp. 621-625.

Stanley, H. E. and Teixeira, J., 1980, "Interpretation of the unusual behavior of H<sub>2</sub>O and D<sub>2</sub>O at low temperatures: Tests of a percolation model," *Journal of Chemical Physics*, Vol. 73(7), pp. 3404-3422.

Sugawara, S. and Katsuta, K., 1966, "Fundamental study of dropwise condensation," *Proc. 3<sup>rd</sup> Int. Heat Transfer Conference*, Vol. 2, pp. 354-361.

Turnbull, D. and Vonnegut, B., 1952, *Ind. Engng. Chem.*, Vol. 44, pp. 1292-1298.

Umur, A. and Griffith, P., 1965, "Mechanism of Dropwise Condensation," *J. Heat Transfer*, Vol. , pp. 275-282.

Vervew, E. J. W. and Overbeek, J. Th. G., 1948, *Theory of Stability of Lyophobic Colloids*, Elsevier, Amsterdam.

Vook, R. W., 1982, "Structure and growth of thin films," *International Metals Review*, Vol. 27(4) , pp. 209-245.

Wayner, P. C. Jr., Kao, Y. K. and La Croix, L. V., 1976, "The Interline Heat-Transfer Coefficient of an Evaporating Wetting Film," *Int. J. Heat Mass Transfer*, Vol. 19, pp. 487-492.

Welch, J. F. and Westwater, J. W., 1961, "Microscopic study of dropwise condensation," *International Developments in Heat Transfer*, ASME, Part II.

Xia, X. and Berkowitz, M. L., 1995, "Electric-field induced restructuring of water at a platinum-water interface: a molecular dynamics computer simulation," *Phys. Rev. Lett.*, Vol. 74(16), pp. 3193-3196.

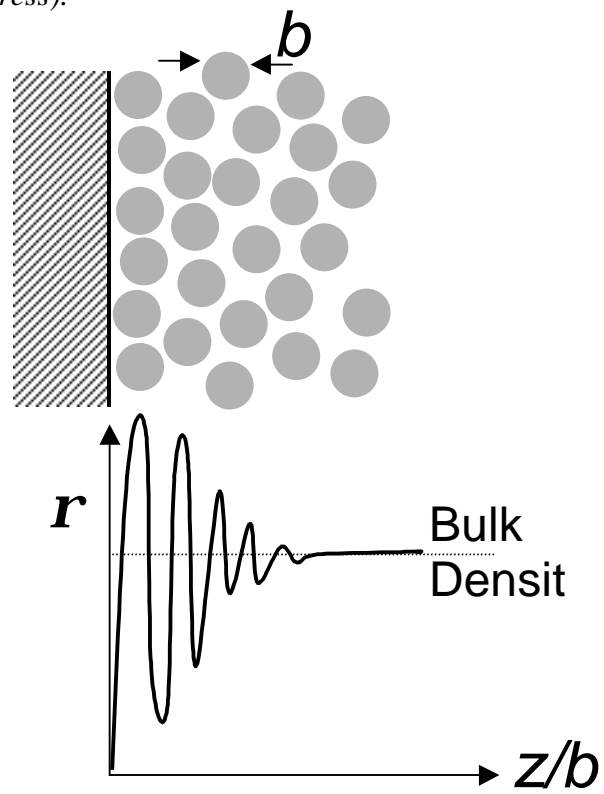


Fig. 1 Schematic diagram of water structure near a crystalline hydrophilic surface

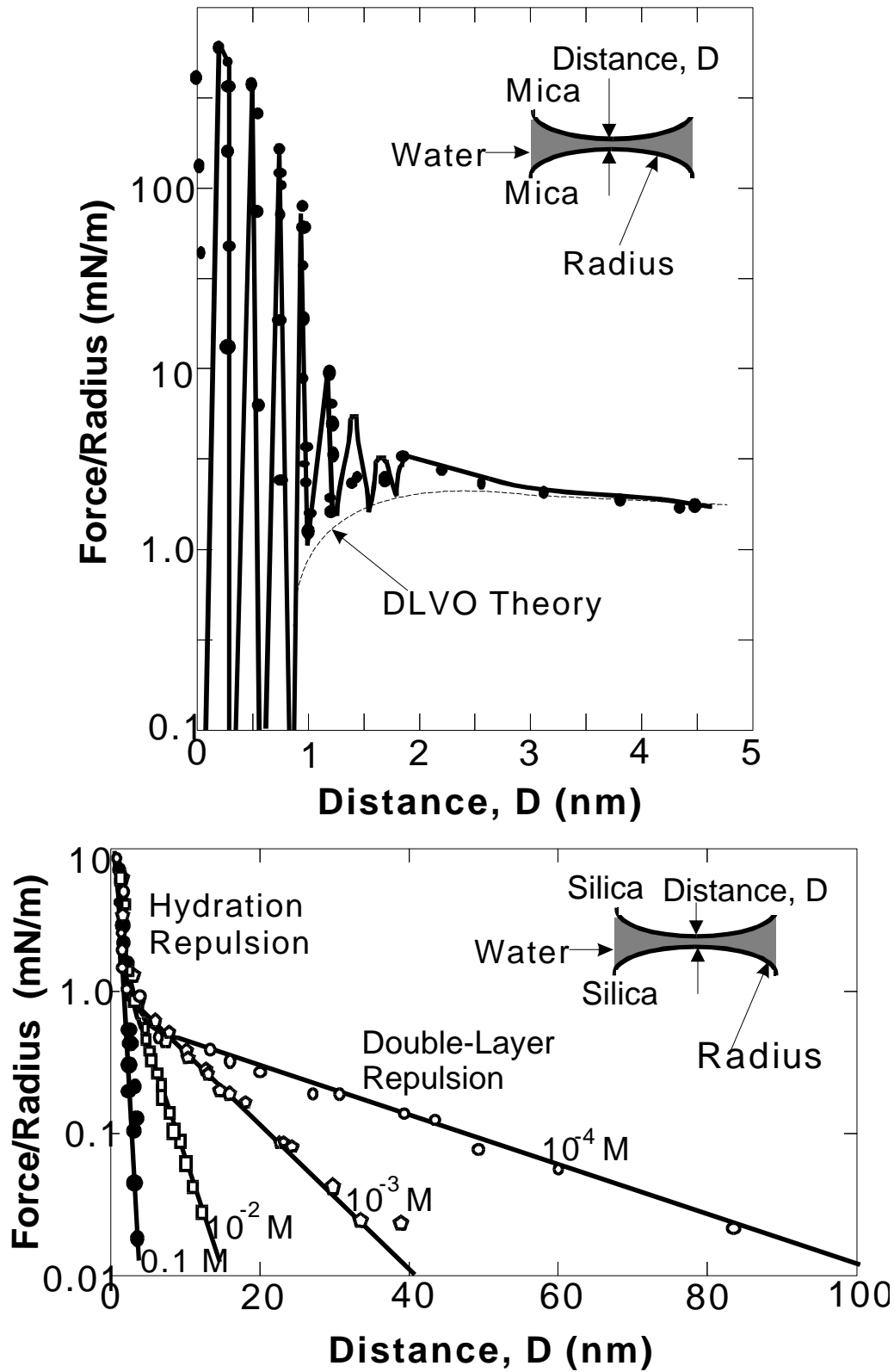
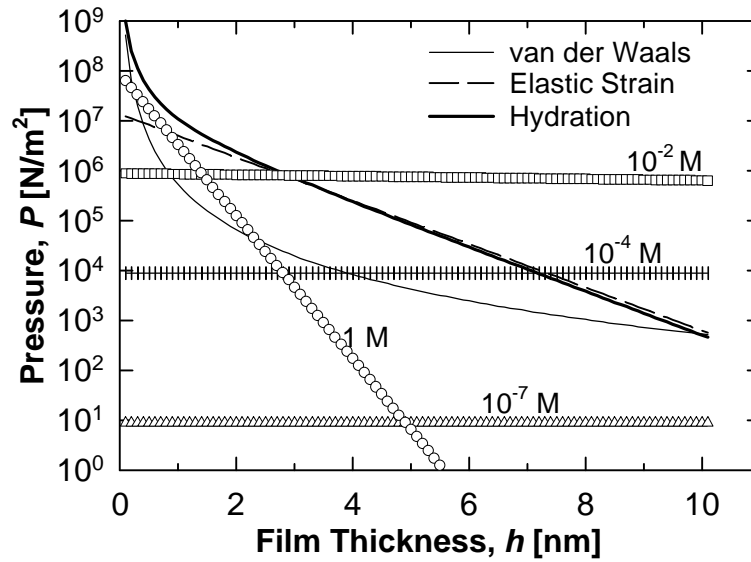


Fig. 2 Repulsive forces measured between two cylinders of (a) mica (Israelachvili and Pashley, 1983) and (b) silica (Horn et al., 1989) surfaces in the presence of water in a surface force apparatus. DLVO theory considers van der Waals and electrostatic forces but not the hydration forces.



**Fig. 3** Comparison of hydration, strain, electrostatic, and van der Waals contributions to the disjoining pressure. The conditions chosen for the calculations were  $l = 1$  nm and  $U = 10$  mJ/m<sup>2</sup> for hydration;  $A = -10^{-20}$  J for van der Waals interaction;  $E = 1.7 \times 10^{10}$  N/m<sup>2</sup> and  $e_o = 0.04$  for strain; and for electrostatic interactions four NaCl electrolyte concentrations,  $10^{-7}$  M (pure water),  $10^{-4}$  M,  $10^{-2}$  M and 1 M, with surface potential is  $f_o = 100$  mV.



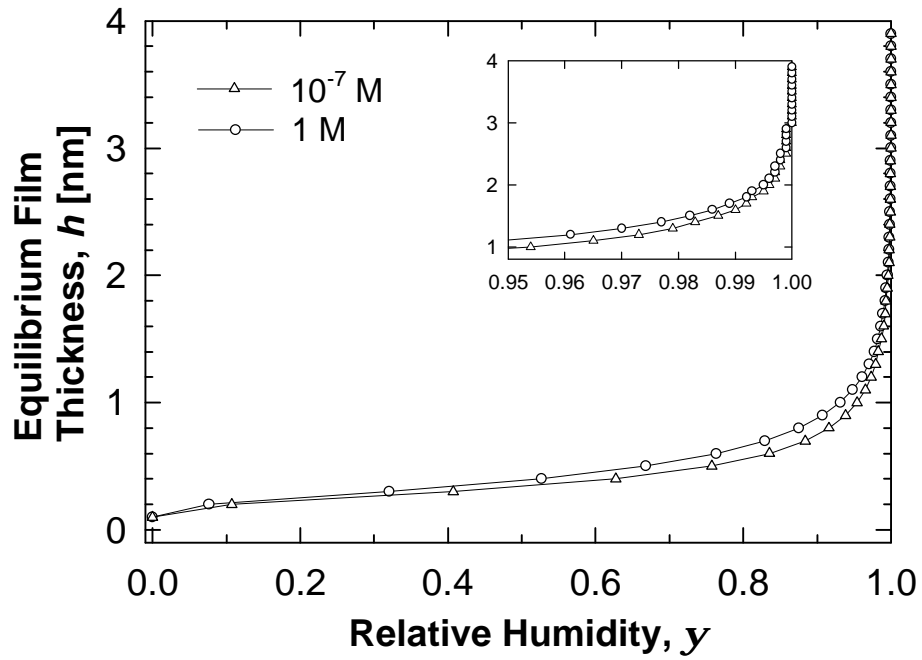


Fig. 4 Equilibrium water film thickness as a function of relative humidity. The conditions were the same as chosen for the predictions in Fig. 3.

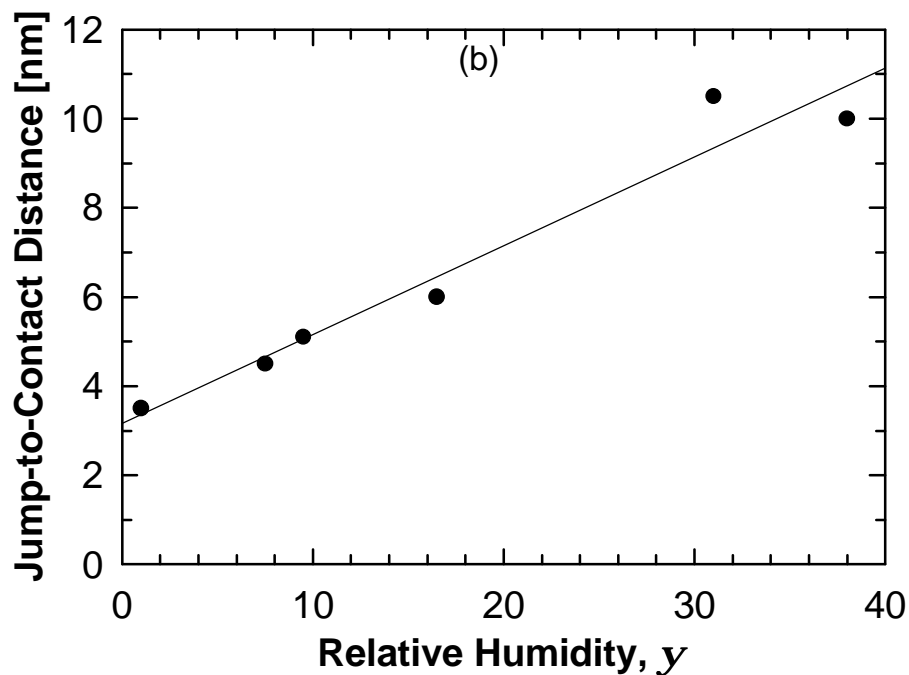
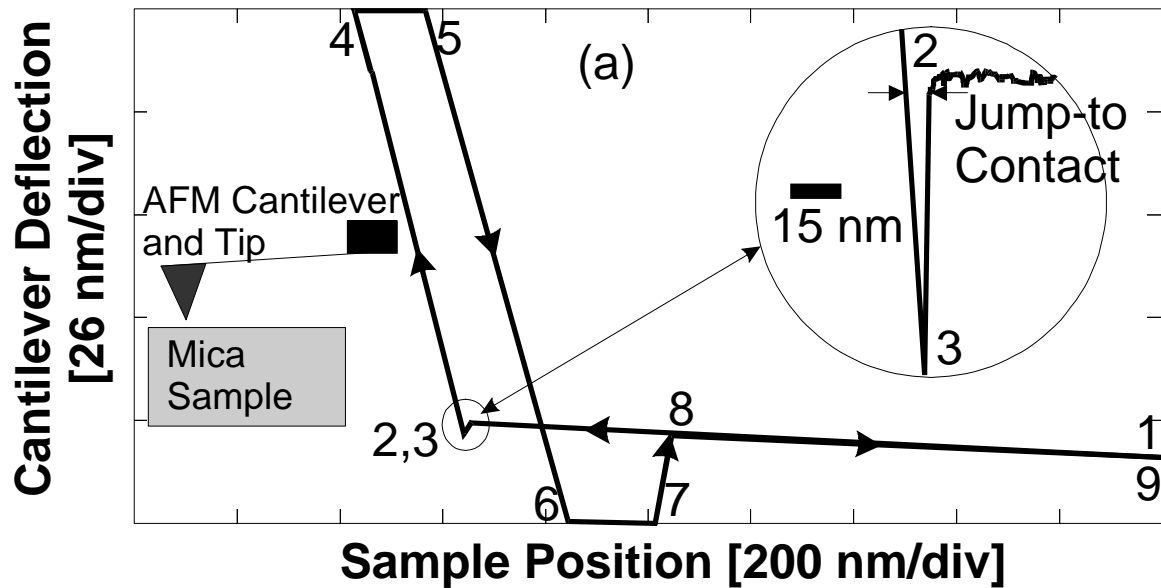


Fig. 5 (a) Deflection of an atomic force microscope (AFM) cantilever tip as a function of sample position during contact with a freshly-cleaved mica surface. 1-2 the sample is moved up towards the AFM tip; 2-3 the tip jumps to contact with the surface due to attractive forces; 3-4 sample is moved up pushing the in-contact cantilever tip; 5-6 sample is retracted away although tip sticks to the surface due to attractive forces; 6-7 tip is still in contact although the signal is out of range; 7-8 cantilever snaps back and out of contact; 8-9 tip is out of contact and remains there as the sample is moved away. (b) Measured jump-to-contact distance as a function of relative humidity.

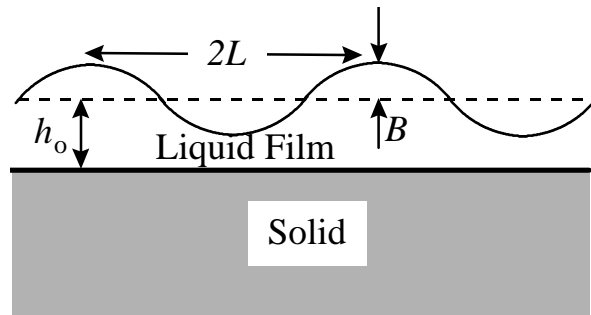


Fig. 6 Perturbation of amplitude  $B$  and wavelength  $2L$  of a liquid film of nominal thickness  $h_o$ .

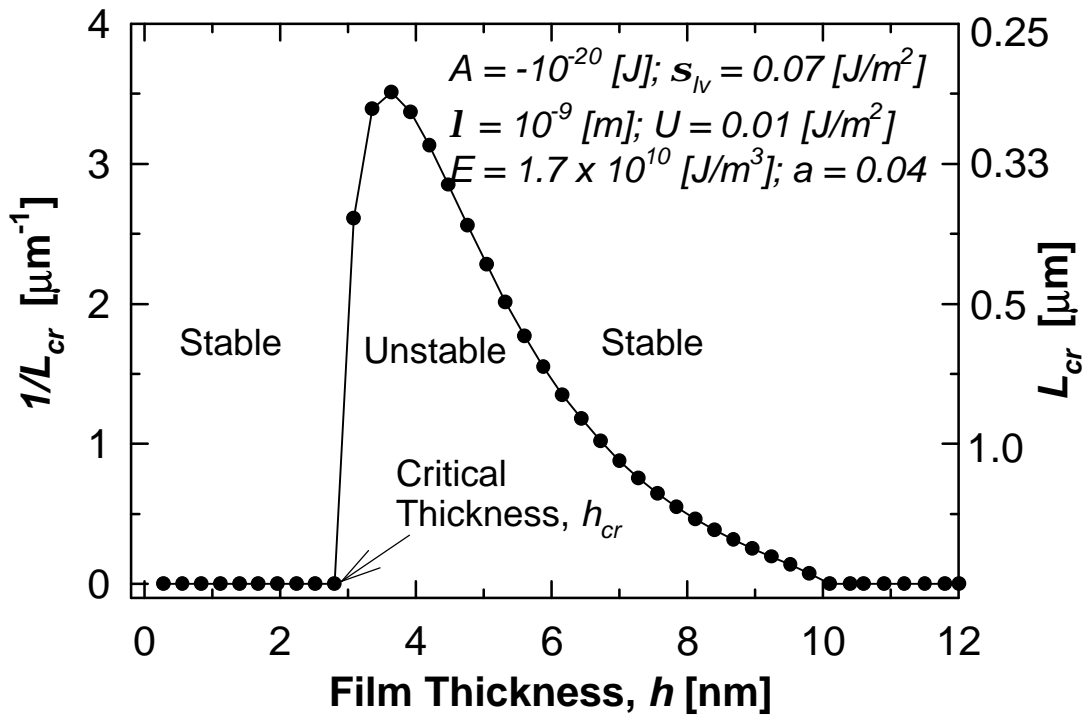


Fig. 7 Stability map of a water film in terms of critical wavelength,  $L_{cr}$ , as a function of film thickness of the water film.

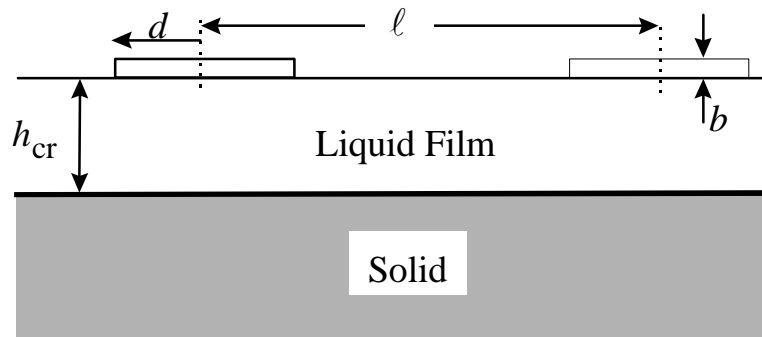


Fig. 8 Schematic diagram showing nuclei of radius  $d$  formed as a monolayer of thickness  $b$  on a water film of critical thickness,  $h_{cr}$ , and separated on an average by a distance,  $\ell$ .

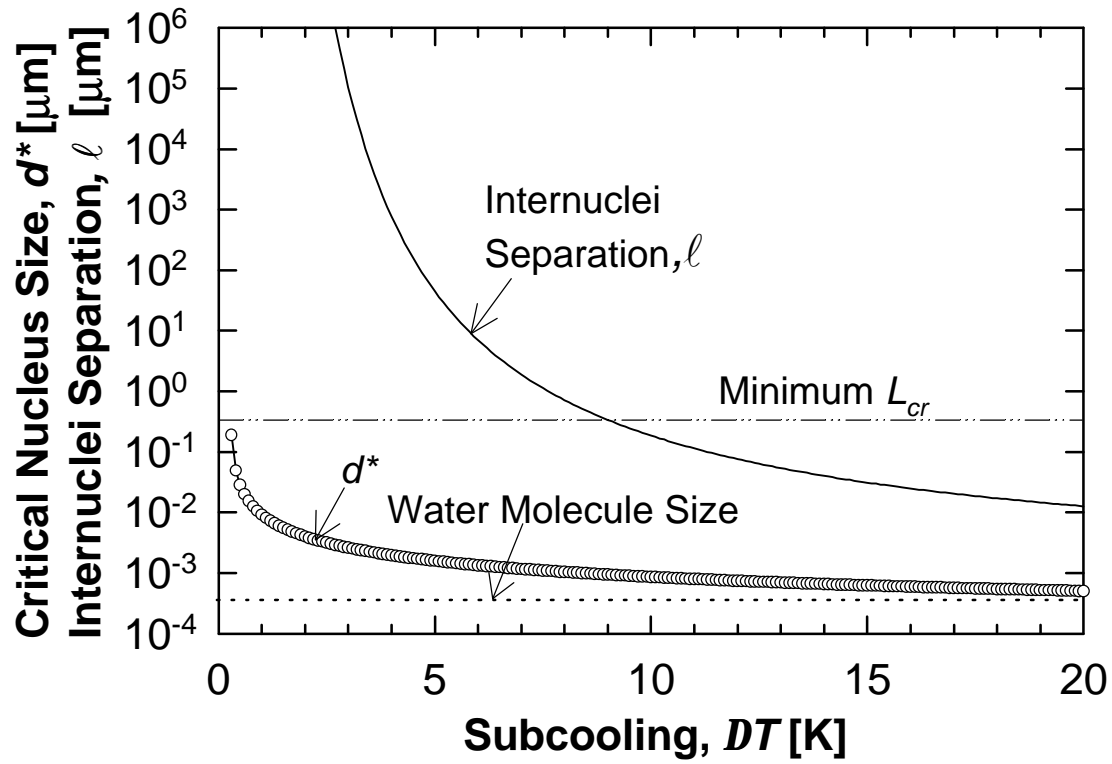


Fig. 9 Prediction of the critical nucleus size and the average internuclei spacing as a function of subcooling for a water film in contact with a hydrophilic surface. The conditions chosen for the hydration, van der Waals, and strain forces are the same as in Fig. 8.